Reprinted from IEEE JOURNAL OF *QUANTUM ELECTRONICS*
Vol. QE-2, Number 9, September 1966
Pp. 507-510

7B1—Ruby Laser Loss Measurement by Comparison of R_1, R_2 Thresholds

D. C. HANNA, W. A. GAMBLING, SENIOR MEMBER, IEEE, AND R. C. SMITH

***Abstract*—A simple method of measuring the losses of a ruby laser resonant cavity has been developed in which the thresholds for R_1 line and R_2 line operation are compared. A quartz birefringent filter is placed in the cavity with quartz disk cut to allow Brewster-angle operation and of such a thickness that the separation between pass bands of the filter analyzer combination is 28 Å. The analyzer, placed between the filter and the output mirror, consists of a stack of fused quartz plates at the Brewster-angle. A known loss is introduced into the cavity by means of a plate inclined to the laser beam at a known angle. With the filter set for R_2 operation the threshold is adjusted to a suitable value by rotating the loss plate to give an attenuation L_2/pass. The filter is then reset for R_1 operation and a different (larger) attenuation L_1 must be introduced by the loss plate to raise the R_1 threshold to the same level. An analysis of the threshold populations of the ^2E levels shows that the losses of the cavity due to all sources of loss other than the loss plate may be obtained from a plot of log L_1, against log L_2.**

INTRODUCTION

MEASUREMENTS OF the oscillation losses of ruby lasers have been reported by a number of authors [1]–[6]. However, all the methods employed are both time consuming and tedious to perform since they involve taking many threshold measurements, which must also (except for the method given in [5]) be taken over the temperature range from liquid nitrogen to room temperature. In addition, the measurements must be fitted to theoretical curves. The derivation of these theoretical curves requires some assumption about the functional relationship between the pump energy and the population of the ^2E levels, and also the assumption, usually implicit, that the ^2E population is uniform along the length of the rod. A method for measuring loss is presented here which can be performed at room temperature, only two threshold measurements being taken, and which does not require the two assumptions mentioned above. It is assumed, however, that the losses are identical for the R_1 and R_2 wavelengths of ruby. This seems reasonable since the two lines are separated by only 14 Å.

The method consists essentially of introducing a known loss L_1 into the laser cavity by means of a glass plate at a known angle, and noting the threshold pump energy for R_1 line operation. The laser is then constrained to operate on the R_2 line by means of a birefringent filter [7] which rejects the R_1 wavelength but passes the R_2 wavelength with negligible attenuation. The plate is adjusted to give a smaller loss L_2 such that the threshold energy for R_2 oscillation is the same as previously obtained for R_1. We now show that the knowledge of L_1 and L_2 is sufficient for the calculation of the remaining cavity losses.

Manuscript received April 14, 1966. This paper was presented at the 1966 International Quantum Electronics Conference, Phoenix, Ariz.

The authors are with the Department of Electronics, Southampton University, Southampton, England.

THEORY

Figure 1 gives the relevant energy levels of pink ruby [6], laser oscillation being obtained between the $\bar{E}(^2E)$ or $2\bar{A}(^2E)$ levels and the $^4A_2$ ground level giving the well-known R_1 and R_2 lines, respectively. The threshold conditions for oscillation on the R_1 and R_2 lines for identical pump energies may be derived as follows.

The populations N_i of each of the levels indicated in Fig. 1 are functions of both the pump energy absorbed E, and the position (x, y, z) inside the ruby, where the x-axis is chosen parallel to the geometrical axis of the rod. Since the $^2T_1$ and ^2E levels are in thermal equilibrium [8], the following relations hold for levels 2 to 6.

$$N_i(x, y, z, E) = N_2(x, y, z, E) \exp(-h\nu_{i2}/kT) \quad (1)$$

where $(i = 2, 3, \cdots, 6)$.

There is negligible population in the $^4T_1$ and $^4T_2$ levels due to fast relaxation from these levels to the ^2E levels so that

$$N_0 = \sum_{i=1}^{6} N_i(x, y, z, E) \quad (2)$$

where N_0 is the total number of chromium ions/cm^3. At 300°K, (1) and (2) can be combined to give

$$N_1(x, y, z, E) + 2.295N_3(x, y, z, E) = N_0 \quad (3)$$

$$N_1(x, y, z, E) + 2.000N_2(x, y, z, E) = N_0. \quad (4)$$

Let R_1 be the double-pass cavity attentuation for R_1 line radiation due to scatter, diffraction, etc., and the reflection loss from the inserted glass plate; let R_2 be the corresponding quantity for the R_2 line. The absorption cross section for the transition $^4A_2 \rightarrow \bar{E}$ will be written as σ_1 and for $^4A_2 \rightarrow 2\bar{A}$ as σ_2. Then, by an extension of Maiman's analysis [9], the threshold condition for oscillation on the R_1 line is

$$\ln R_1 = 2 \int_0^l [N_1(x, y, z, E) - 2N_2(x, y, z, E)]\sigma_1 \, dx \quad (5)$$

where l is the length of the ruby rod and integration is carried out along the lasing filament. The factor 2 before $N_2(x, y, z, E)$ results from the different statistical weights of the $^4A_2$ and $\bar{A}$ levels.

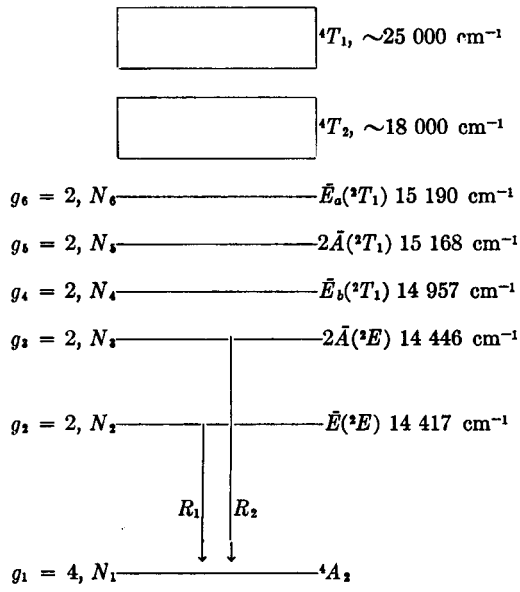

Fig. 1. Energy level diagram of Cr^{3+} in Al_2O_3. Statistical weights and populations are given on the left.

Similarly, the threshold condition for R_2 oscillation is

$$\ln R_2 = 2\int_0^l [N_1(x, y, z, E) - 2N_3(x, y, z, E)]\sigma_2\, dx, \quad (6)$$

integration being again carried out along the lasing filament.

$N_1(x, y, z, E)$ can be eliminated from (5) by means of (4), and from (6) by means of (3) to give

$$\ln R_1 = 2\sigma_1 N_0 l - 8\int_0^l \sigma_1 N_2(x, y, z, E)\, dx \quad (7)$$

$$\ln R_2 = 2\sigma_2 N_0 l - 2 \times 4.295 \int_0^l \sigma_2 N_3(x, y, z, E)\, dx. \quad (8)$$

With a loss plate inserted in the cavity, R_1 and R_2 can be varied so that the threshold equations (7) and (8) for R_1 and R_2 line oscillation are satisfied at exactly the same pump energy E_1.

But from (1), at 300°K,

$$N_3(x, y, z, E_1) = 0.87N_2(x, y, z, E_1) \quad (9)$$

and substituting this expression for $N_3(x, y, z, E)$ in (8),

$$\ln R_2 = 2\sigma_2 N_0 l - 2 \times 4.295 \times 0.87 \cdot \int_0^l \sigma_2 N_2(x, y, z, E_1)\, dx. \quad (10)$$

If threshold laser action on the R_2 line takes place in the same filament as for R_1, then we can equate $\int_0^l N_2(x, y, z, E_1)$ in (7) and (10) to give

$$\frac{\ln R_1 - 2N_0\sigma_1 l}{4\sigma_1} = \frac{\ln R_2 - 2N_0\sigma_2 l}{0.87(4.295\sigma_2)}. \quad (11)$$

So far no account has been taken of the absorption of R_1 and R_2 light by Cr^{3+} ions in excited states. It has been pointed out by Nelson and Remeika [6] that such an absorption would constitute an oscillation loss. Unfortunately, the magnitude of this loss is uncertain since a wide range of values have been reported [10]–[14] for the absorption cross section from the excited levels. Following the same argument as that of Nelson and Remeika, we define a cross section σ_u which is the average absorption cross section for σ-polarized R_1 light by chromium ions residing in the excited states 2, 3, ⋯ , 6. σ_u will be assumed equal for the R_1 and R_2 wavelengths. The absorption coefficient from the excited levels for R_1 or R_2 light is then

$$\sum_{i=2}^{6} N_i(x, y, z, E)\sigma_u. \quad (12)$$

But from (1), at 300°K

$$\begin{aligned}\sum_{i=2}^{6} N_i(x, y, z, E) &= 2.000N_2(x, y, z, E) \\ &= 2.295N_3(x, y, z, E)\end{aligned} \quad (13)$$

and the absorption in (12) can be included in (7) and (8) to give

$$\ln R_1 = 2\sigma_1 N_0 l - 8\int_0^l \sigma_1 N_2(x, y, z, E)\, dx + 2.000\sigma_u \int_0^l 2N_2(x, y, z, E)\, dx \quad (14)$$

and

$$\ln R_2 = 2\sigma_2 N_0 l - 2 \times 4.295 \int_0^l \sigma_2 N_3(x, y, z, E)\, dx + 2 \times 2.295 \int_0^l \sigma_u N_3(x, y, z, E)\, dx. \quad (15)$$

Hence, (11) now becomes

$$\frac{\ln R_1 - 2N_0\sigma_1 l}{4\sigma_1 - 2\sigma_u} = \frac{\ln R_2 - 2N_0\sigma_2 l}{0.87(4.295\sigma_2 - 2.295\sigma_u)}. \quad (16)$$

Let δ_1 be the single-pass attenuation of R_1 light due to scatter, diffraction, and mirror losses, and L_1 the single-pass attenuation of R_1 light due to the loss plate. If δ_2 and L_2 are the corresponding quantities for R_2 light then

$$R_1 = \delta_1^2 L_1^2 \quad (17)$$

$$R_2 = \delta_2^2 L_2^2. \quad (18)$$

Substituting (17) and (18) into (16) we obtain

$$\frac{\ln L_1 + \ln \delta_1 - N_0\sigma_1 l}{4\sigma_1 - 2\sigma_u} = \frac{\ln L_2 + \ln \delta_2 - N_0\sigma_2 l}{0.87(4.295\sigma_2 - 2.295\sigma_u)}. \quad (19)$$

The unknowns are δ_1 and δ_2, and if, as discussed above, the assumption is made that, $\delta_1 = \delta_2 = \delta$, say then δ can be calculated from (19).

Apparatus

The experimental arrangement is shown in Fig. 2. The laser head, which can accommodate Brewster-angled or plane-ended, two-inch rubies, consists of a multilayer dielectric-coated elliptical cylinder. The ruby is pumped by a linear two-inch flash tube which is energized by a

capacitor bank of 200 μF. The dielectric-coated mirrors have a reflectivity of better than 99 percent and are separated by a distance of 40 cm.

The use of a birefringent filter to obtain R_2 line operation has been described by Hubbard and Fisher [7] but the technique used here differs in some details. For simplicity of description we shall assume that a 90° cut ruby is used, although this is not necessary for the experiment. The natural quartz retardation plate is cut to allow Brewster-angle operation and is of such a thickness that the separation between pass bands of the filter/analyzer combination is 28 Å, twice the R_1–R_2 separation. Tuning of the filter is achieved by rotating the disk about an axis parallel to the c-axis of the ruby [16], a rotation of 51 minutes changing the filter from R_1 pass to R_2 pass. Temperature tuning is also possible [7] and the range of temperature required is about 20°C. To avoid detuning due to ambient temperature changes, the work was carried out in a room whose temperature was stabilized to $\pm 1/4$°C.

The analyzer consists of a stack of fused quartz plates at the Brewster angle [17]. The single-pass optical path through the retardation plate is twice that used by Hubbard and Fisher and the analyzer plates are therefore used in double pass, reducing the number of plates required.

The ordinary and extraordinary rays in the quartz propagate in slightly different directions, the calculated angle between them being 13 minutes. The imperfect recombination of the two rays is a source of loss since light leaving the quartz will not be 100 percent linearly polarized perpendicular to the ruby c-axis. However, measurement has shown that when the filter is tuned for R_1 or R_2, less than 1 percent of the laser radiation leaving the quartz is polarized parallel to the c-axis. Hence, the insertion loss of the filter is less than 1 percent at the pass wavelength.

The known loss is introduced into the cavity by means of a fused quartz plate inclined to the laser beam at a known angle. The plate is wedged by about 3 minutes to prevent its acting as a Fabry–Perot etalon. The axis of rotation of the loss plate is perpendicular to the c-axis whereas the analyzer can be rotated about an axis parallel to the c-axis. It is necessary to know the refractive index of the plate and the angle of incidence accurately, particularly at large angles of incidence.

Measurement

For various values of the threshold energy, corresponding values of L_1 and L_2 are obtained. From (19) it can be seen that a plot of ln L_1 against ln L_2 should give a straight line with gradient

$$G = \frac{4\sigma_1 - 2\sigma_u}{0.87(4.295\sigma_2 - 2.295\sigma_u)}. \quad (20)$$

Substituting G from (20) in (19) gives

$$\ln L_1 = G \ln L_2 + (G - 1) \ln \delta + N_0 l(\sigma_1 - G\sigma_2). \quad (21)$$

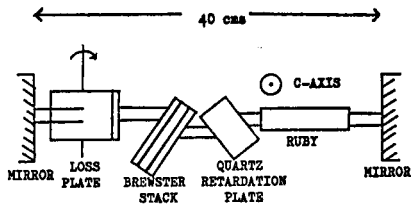

Fig. 2. Laser cavity with birefringent filter and loss plate.

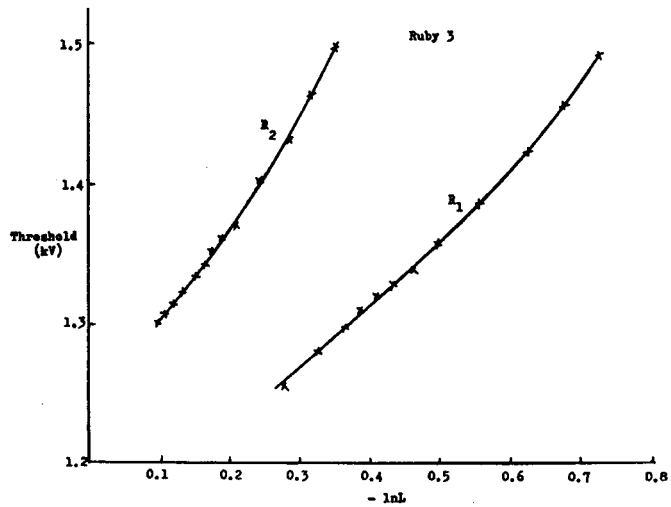

Fig. 3. Dependence of threshold (expressed as the voltage across the capacitor bank) on inserted loss for both R lines.

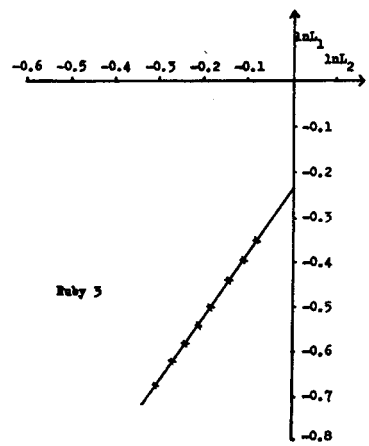

Fig. 4. Plot of ln L_1 against ln L_2.

TABLE I

Ruby	Doping Percent Cr^{3+}	Geometry & Finish	G	Percent Loss Per Pass
1	0.03	both ends flat, polished side	1.43	37
2	0.05	both ends flat, polished side	1.44	46
3	0.027	both ends flat, rough side	1.45	31
4	0.03	Brewster ends, rough side	1.47	15

From the gradient and the intercept on the ln L_1 axis, and knowing N_0, l, σ_1, σ_2, the loss δ can be found. Figures 3 and 4 show the results from a typical experiment. Figure 3 gives the threshold voltage for oscillation on R_1 or R_2 for various values of inserted loss. From the curves in Fig. 3 the values of ln L_2 and ln L_1 corresponding to the same threshold energy can be found, and from this information Fig. 4 has been obtained. Four rubies of different geometries and dopings have been measured and the results are given in Table I.

Discussion

For all four rubies the plot of ln L_1 against ln L_2 gave a straight line and, within experimental error, the gradient of this line is the same for all the rubies, as predicted by (19), thus confirming the threshold model used here. The value of the gradient is 1.45 with an estimated accuracy of ± 0.05. Substituting this in (21) and using the values $\sigma_1 = 2.0 \times 10^{-20}$ cm^2 and $\sigma_2 = 1.45 \times 10^{-20}$ cm^2 calculated from the data of Nelson and Sturge [8], (21) becomes

$$\ln L_1 = 1.45 \ln L_2 + 0.45 \ln \delta - 1.03 \times 10^{-21} N_0 l. \quad (22)$$

Thus, for any ruby, knowing the doping and the length, the loss δ can be found by measuring just one pair of corresponding values of L_1 and L_2 and then substituting these values in (22).

A valuable feature of this technique of loss measurement is that it gives the cavity loss δ separated from any loss due to absorption from excited levels. It also gives some information about the value of σ_u. By inserting the experimentally obtained value $G = 1.45 \pm 0.05$ and the values of σ_1 and σ_2 quoted previously into (20), it is found that the upper limit for σ_u is 2.5×10^{-21} cm^2. This is about one-quarter of the value extrapolated from the data of Gires and Mayer [10], [11] and is in agreement with more recent measurements [12]–[15].

It is difficult to estimate the absolute accuracy of the results in the last column of Table I. They have all been calculated using the value $G = 1.45$ in (21). However, δ is sensitive to the value of the term $\sigma_1 - G\sigma_2$ in (21) (since $\sigma_1 \sim G\sigma_2$), and this, in turn, is sensitive to the values of G and σ_1/σ_2. A more accurate estimate of G than we have obtained experimentally is needed, and an accurate calculation of G from (20) requires a more precise knowledge of σ_u than the most reliable value so far available, $(3 \pm 1) \times 10^{-21}$ cm^2, given by Kiang et al. [12]. Regardless of the exact choice of G in (21), however, the technique does give an accurate comparison of the relative losses of different rubies.

Conclusion

A technique for ruby loss measurement has been developed which is simple to perform and needs a minimal amount of calculation from the raw experimental data. Since explicit knowledge of the functions $N_i(x, y, z, E)$ is not required, the technique can be applied to any ruby regardless of geometry and pumping scheme. The loss δ so obtained is the cavity loss as distinct from any loss due to excited state absorption.

Three assumptions have been used in the analysis. The first is that the cavity loss δ is the same for R_1 and R_2. This would only be violated if there were a sharp impurity absorption line (not due to Cr^{3+}) coinciding with just one of the R lines. The second assumption is that threshold laser action on the R_2 line takes place in the same filament as for R_1. The validity of this assumption is a consequence of the first assumption since which ever filament is least lossy for R_1 should also be least lossy for R_2. However, as an additional check, confirmation of this has been made in photographs taken of the ruby face while laser action was taking place. The last assumption was that σ_u is the same for R_1 and R_2 light. The measurements of Kiang et al. [12] show that σ_u is only changing slowly with wavelength at 6900 Å. Exact measurement of σ_u at 6943 Å (R_1) or 6929 Å (R_2) is difficult since R line fluorescence causes some uncertainty. However, this last assumption would only be violated by the fortuitous coincidence of an excited level absorption line with either the R_1 or R_2 wavelength.

References

[1] R. J. Collins and D. F. Nelson, "The pulsed ruby optical maser," *Proc. 1961 Conf. on Optical Instruments*, pp. 441–454.
[2] J. I. Masters, "Estimation of ruby laser oscillation loss," *Nature*, vol. 199, pp. 442–443, August 1963.
[3] R. L. Aagard, "Losses in a pulsed ruby laser," *J. Opt. Soc. Amer.*, vol. 53, pp. 911–914, August 1963.
[4] D. Chen, "Measurements of cavity loss in a pulsed ruby laser," *Nature*, vol. 205, pp. 271–272, January 1965.
[5] V. Daneu, C. A. Sacchi, and O. Svelto, "$\bar{E}$-level population of ruby vs. pumping," *Appl. Opt.*, vol. 4, pp. 863–866, July 1965.
[6] D. F. Nelson and J. P. Remeika, "Laser action in a flux-grown ruby," *J. Appl. Phys.*, vol. 35, pp. 522–529, March 1963.
[7] C. J. Hubbard and E. W. Fisher, "Ruby laser action at the R_2 wavelength," *Appl. Opt.*, vol. 3, pp. 1499–1500, December 1964.
[8] D. F. Nelson and M. D. Sturge, "Relation between absorption and emission in the region of the R lines of ruby," *Phys. Rev.*, vol. 137, pp. A1117–A1130, February 1965.
[9] T. H. Maiman, R. H. Hoskins, I. J. d'Haenens, C. K. Asawa, and V. Evtuhov, "Stimulated optical emission in fluorescent solids, (1) Theoretical considerations," *Phys. Rev.*, vol. 123, pp. 1145–1150, August 1961.
[10] F. Gires and G. Mayer, "Mesures du spectre d'absorption d'un rubis excité pour l'étude de son fonctionnement en maser optique," *Compt. Rend. Acad. Sci., Paris*, vol. 254, pp. 659–661, January 1962.
[11] F. Gires and G. Mayer, "Propriétés optiques du rubis fortement excité," *Ann. Radioélect.*, vol. 28, pp. 112–122, April 1963.
[12] Y. C. Kiang, J. F. Stephany, and F. C. Unterleitner, "Visible spectrum absorption cross section of Cr^{3+} in the $^2\bar{E}$ state of pink ruby," *IEEE J. of Quantum Electronics*, vol. QE-1, pp. 295–298, October 1965.
[13] T. Kushida, "Infrared absorption spectra from excited states in ruby," *J. Phys. Soc. Japan*, vol. 20, p. 619, April 1965.
[14] ——, "Absorption spectra of ruby in excited states," presented at the 1965 Spring meeting of the Physical Society of Japan.
[15] F. Gires and G. Mayer, private communication.
[16] J. A. Calviello, E. W. Fisher, and Z. H. Heller, "Simultaneous laser oscillation at R_1 and R_2 wavelengths in ruby," *IEEE J. of Quantum Electronics (Correspondence)*, vol. QE-1, p. 132, June 1965.
[17] G. Weiser, "A rigid low-loss polarizing device for giant pulse lasers using Brewster angle polarization," *Proc. IEEE (Correspondence)*, vol. 52, p. 966, August 1964.